PAPER

Check for updates

Guest-induced magnetic exchange in paramagnetic [M₂L₄]⁴⁺ coordination cages†

Mukesh K. Singh, iD * Alvaro Etcheverry-Berríos, iD Julia Vallejo, Sergio Sanz, iD José Martínez-Lillo, iD ‡ Gary S. Nichol, iD Paul J. Lusby iD * and Euan K. Brechin iD *

Paramagnetic complexes that possess magnetically switchable properties show promise in a number of applications. A significantly underdeveloped approach is the use of metallocages, whose magnetic properties can be modulated through host–guest chemistry. Here we show such an example that utilises a simple [Cu^{II}₂L₄]⁴⁺ lantern complex. Magnetic susceptibility and magnetisation data shows an absence of exchange in the presence of the diamagnetic guest triflate. However, replacement of the bound triflate by ReBr₆²⁻ switches on antiferomagnetic exchange between the Cu and Re ions, leading to an $S = 1/2$ ground state for the non-covalent complex [ReBr₆²⁻⊂Cu^{II}₂L₄]²⁺. Comparison of this complex to a "control" palladium-cage host–guest complex, [ReBr₆²⁻⊂Pd^{II}₂L₄]²⁺, shows that the encapsulated ReBr₆²⁻ anions retain the same magnetic anisotropy as in the free salt. Theoretically calculated spin-Hamiltonian parameters are in close agreement with experiment. Spin density analysis shows the mode of interaction between the Cu^{II} and Re^{IV} centres is through the Re-Br···Cu pathway, primarily mediated through the Cu(d$_{x^2-y^2}$)|Br$_{sp}$|Re(d$_{yz}$) interaction. This is further supported by overlap integral calculations between singly occupied molecular orbitals (SOMOs) of the paramagnetic ions and natural bonding orbitals analysis where considerable donor-to-acceptor interactions are observed between hybrid 4s4p orbitals of the Br ions and the empty 4s and 4p orbitals of the Cu ions.

Introduction

Amongst the many hundreds of coordination cages to appear in the past 30 years, the Pd₂L₄ topology, first described by Steel,[1] is the simplest, arguably the most versatile and one of the most well-studied.[2–7] It has been investigated in multiple contexts, as it's host–guest chemistry can be tuned to bind anions,[8] as well as neutral species.[9,10] This versatility has allowed it to be exploited for a number of applications that involve the binding of drug[5] and imaging molecules,[11] as well as substrates for catalysis.[12,13] Paramagnetic M₂L₄ lantern cages are much less well explored,[14] indeed investigations of the magnetic behaviour of any supramolecular cages remains virtually unexplored.[15] However, the host–guest chemistry of

these systems offers a range of potential advantages for the exploitation of magnetic materials properties. These include, for example, the reversible inducement of magnetic exchange interactions, the encapsulation of unstable/reactive molecules or those with unusual geometries/coordination numbers, solid-state dilution, and the tuning of magnetic anisotropy. Such properties are sought-after for the construction of single-ion[16] and single-molecule magnets,[17] electron–spin based qubits,[18] and may find application in magnetic sensing, switching and molecular recognition.[19] Functionalisation of the organic framework would also aid surface deposition and the transformation of 0D molecular cages to 2D sheets and/or 3D MOFs imbued with the same physical properties.

Successful ingress of a magnetic guest into a magnetic host may have little effect on magnetic properties if there are no significant interactions between the two, nor any geometrical change in either component. However, this is unlikely if size/symmetry/electrostatic matching is efficient. Encapsulation may solely induce structural changes to the host/guest and this has previously been shown to have significant impact upon, for example, the magnetic anisotropy of 3d transition metal ions in magnetic MOFs,[20] and the high spin–low spin transition temperature in spin crossover materials.[21] Indeed, recent studies of single-ion magnets have shown how crucial

EaStCHEM School of Chemistry, The University of Edinburgh, David Brewster Road, Edinburgh, EH9 3FJ Scotland, UK. E-mail: msingh2@exseed.ed.ac.uk, Paul.Lusby@ed.ac.uk, ebrechin@ed.ac.uk

geometry is in determining magnetisation relaxation dynamics,[22] and thus metallosupramolecular cages could play a key role here if their internal cavity can be designed to suit a specific d/f metal ion geometry. Covalent bonding through an intervening organic/inorganic ligand or a short dipolar interaction between the metal ions in the host and guest will mediate a magnetic exchange interaction, the sign and strength of which can be controlled by the nature of the linker and the identity of the metal ions. This then allows for control over the magnetic ground/excited states of the cage, the manipulation of which underpins application in a breadth of technologies.[23]

Interesting potential guest molecules include the rhenium(IV) hexahalides, $[ReX_6]^{2-}$, that possess very large spin–orbit coupling constants ($\lambda \sim 1000$ cm^{-1} in the free ion) that results in significant magnetic anisotropy. In addition, spin delocalisation of the electron density from the metal to the halide imparts significant Re–X···X–Re intermolecular exchange interactions which can be strong enough to induce magnetic order in the salts of these anions at relatively high temperatures.[24,25] For example, $K_2[ReBr_6]$ shows antiferromagnetic order below 14 K.[26] Here we show that the $[ReBr_6]^{2-}$ anion can be encapsulated inside a paramagnetic $[Cu^{II}_2L_4]^{4+}$ (L = 1,3-bis(3-ethynylpyridyl)benzene) cage by reporting the synthesis and characterisation of three related species, $[Cu_2L_4(H_2O)(OTf)_3](OTf)\cdot MeCN$ (**1**), $ReBr_6 \subset [Pd^{II}_2L_4](BF_4)_2$ (**2**) and $ReBr_6 \subset [Cu^{II}_2L_4(OTf)_2]$ (**3**).

Results and discussion

All three cages, **1–3**, are made from the self-assembly of four molar equivalents of ligand molecule L with two molar equivalents of the corresponding metal salt (**1**), followed by one molar equivalent of guest (**2–3**) (see the ESI for full details†). Complex formation was confirmed by electrospray ionization mass spectrometry (ESI–MS), the spectra showing **1–3** remain intact in solution (Fig. S1–S3†). The ^1H spectra of $[Pd^{II}_2L_4](BF_4)_4$ shows the expected seven signals,[3,27] while the ^1H spectra of the host–guest complex **2** show only five signals (Fig. S4–S6†). The missing signals correspond to the cavity protons (H_a and H_e) that strongly interact with the paramagnetic guest (H···Br–Re, distances in the range $H_a\cdots Br$ 2.46–3.03 Å and $H_e\cdots Br$ 2.99–3.25 Å). The hydrodynamic radii determined by ^1H NMR DOSY experiments for both $[Pd^{II}_2L_4](BF_4)_4$ and the host–guest complex (**2**) are ~10 Å, confirming that the guest has been encapsulated in the host cavity (Fig. S7†).

Single crystal X-ray crystallography (see the ESI for full details†) reveals that **1–3** crystallise in triclinic (**1**, **2**) and monoclinic (**3**) crystal systems and structure solution was performed in the $P\bar{1}$ (**1**, **2**) and $P2_1/c$ (**3**) space groups (Table S1†). All three cages possess the same general structure (Fig. 1, Tables S2–S4†), with the host framework conforming to the well-known lantern-like $[M_2L_4]^{4+}$ cage. The Cu^{II} ions in **1** are six coordinate and in Jahn–Teller (JT) distorted octahedral geometries (Cu–N$_L$ = 1.99–2.06 Å; Cu–O = 2.32–2.62 Å; *cis*, 87–94°; *trans*, 176–177°), with triflate ions bonded in the outward facing apical sites and a combination of a single triflate and a water molecule bound in the inward facing apical positions, presumably because two internally bound anions would be prohibited due to space constraints. Charge balance is maintained through the presence of an additional triflate anion that lies outwith the cage, but with close contacts to both the Ph groups of the ditopic ligand, L (C(H)···O/F, 3.2–3.6 Å) and to the apical OTf molecule (O/F···O/F, 2.6–2.9 Å). The sole MeCN
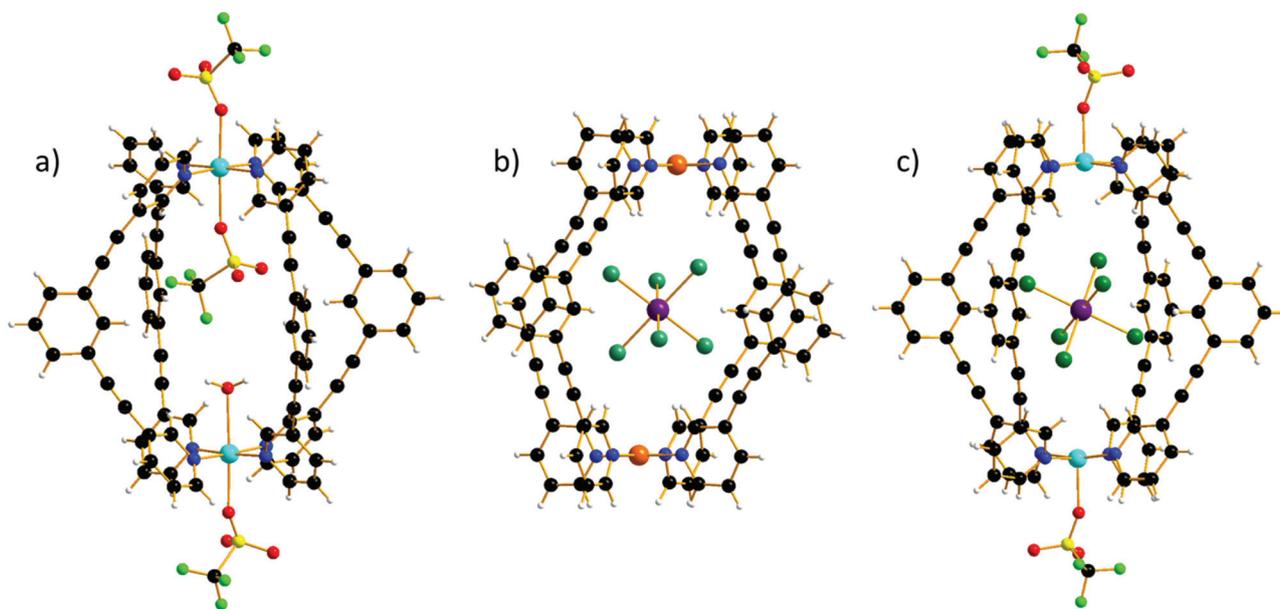

Fig. 1 Molecular structures of (a) **1**, (b) **2** and (c) **3**. Colour code: Cu = light blue, C = black, N = dark blue, O = red, S = yellow, F = light green, H = white, Pd = orange, Br = dark green, Re = purple. Solvents and additional counter anions omitted for clarity.

of crystallisation is H-bonded to the H_2O molecule $(O(H) \cdots N$, 2.97 Å) and therefore partially occupies the cavity of cage, protruding out between two L ligands. The L ligands of neighbouring cages interdigitate with $C(Ph) \cdots C(Ph)$ distances >3.5 Å which, alongside the distorted/flexible Cu geometry and the presence of anions/solvents, may account for the severe twisting of the L ligand geometry (Fig. S8†) enforcing a reduction from the pseudo tetragonal symmetry of the $[Pd_2L_4]^{4+}$ cage. From analysis of the extended structures in **2–3**, it is clear that both the guest anion and the crystallographic symmetry also play a key role in dictating molecular symmetry (Fig. S9†). For example, there are two orientations of the cage in **3** compared to one orientation in all the other cages and no uncoordinated anions, leading to a distinctly different packing arrangement in the crystal.

There are multiple close contacts between the *ortho* protons of both the pyridine and phenyl moieties of L and the Br ions of the guest (C–H···Br–Re, ~2.5–3.7 Å), in agreement with the NMR data. The Cu^{II} ions in **3** are 5-coordinate and square pyramidal in geometry $(Cu–N_L = 2.01$ Å; Cu–O = 2.24 Å; *cis*, 88–98°; *trans*, 168–174°), with the triflate ions bonded in the outward facing apical sites and the Br ions of the guest occupying the positions sitting below the square plane of the Cu^{II} ion $(Cu \cdots Br, \sim4.3$ Å). The Cu···Cu distance is now ~12.2 Å compared to ~11.5 Å in **1**, again reflecting the increased interactions between host–guest when the $ReBr_6^{2-}$ anion is introduced.

Magnetic properties

Direct current magnetic susceptibility (χ) and magnetisation (*M*) data for **1–3** were measured in the *T* = 270–2 K, *B* = 0.1 T and *T* = 2–7 K, *B* = 0.5–5.0 T temperature and field ranges, respectively. These are plotted as the χT product *versus T* and *M versus B* in Fig. 2. For the quantitative interpretation of the magnetic properties of **1–3** we used spin-Hamiltonian (1):

$$\hat{H} = D[\hat{S}_{Z,Re}^2 - S_{Re}(S_{Re}+1)/3] + \mu_B B \sum_i g_i \hat{S}_i - 2\sum_{i<j} J_{i,j} \hat{S}_i \cdot \hat{S}_j$$

(1)

where the first term corresponds to the single ion axial anisotropy of the Re^{IV} ion, the second term is the Zeeman effect of the applied magnetic field, and the third term the exchange interaction between the constituent (Cu^{II}, Re^{IV}) metal centres. The χT product and the variable temperature variable field magnetisation data for **1–3** were simultaneously fitted to spin-Hamiltonian (1), affording the best fit parameters collected in Table 1.

In complex **1**, the two Cu^{II} ions sit at a distance of ~11.5 Å and even though they are connected by a conjugated organic ligand (L) one would not expect to see any significant magnetic interaction between them. This is reflected in the χT data which is invariant with temperature, and both the susceptibility and magnetisation data can be simultaneously fitted with $J_{Cu–Cu}$ = 0.0 cm^{-1} with g_{Cu} = 2.095. The susceptibility and magnetisation data for **2** are near identical to those reported in the literature
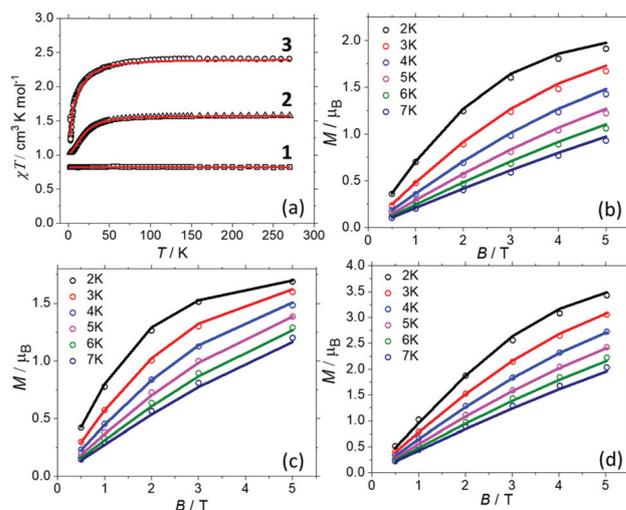
Fig. 2 (a) Magnetic susceptibility data for **1–3** measured in an applied field, *B* = 0.1 T. (b–d) Magnetisation data for **1–3**, respectively, in the *T* = 2–7 K range in fields up to, *B* = 5 T. The solid lines represent the simultaneous fits of the susceptibility and magnetisation data to spin-Hamiltonian (1). See the main text and Table 1 for the best fit parameters.

Table 1 Experimental and calculated best fit parameters for the magnetic exchange (*J*) and axial zero-field splitting (D_{Re}) parameters in complexes **1–3**

| | **1** | **2** | **3** | |
	Expt	*Expt*	*Expt*	*Calc*
J_{CuRe}/cm^{-1}	—	—	−0.45(1)	−0.15
J_{CuCu}/cm^{-1}	0.0	—	0.0	0.0
D_{Re}/cm^{-1}	—	+21.9(1)	+21.9(1)	+23.0
g_{Cu}	2.095	—	2.095(1)	2.162
g_{Re}	—	1.832(1)	1.832(1)	1.749

for $[ReBr_6]^{2-}$ salts.[24] This is to be expected since there has been little distortion to its geometry upon encapsulation, as shown in the overlay plots in Fig. S10† and shape analysis (Table S5†).[28] Thus a simultaneous fit of the susceptibility and magnetisation data affords g_{Re} = 1.832, D_{Re} = +21.9 cm^{-1}, in agreement with both previously published experimental[24] and theoretical values.[29] In order to the fit the data for **3**, the g_{Cu}, g_{Re} and D_{Re} from the fits of compounds **1** and **2** were fixed, and only the $J_{Cu–Re}$ interaction allowed to vary. A simultaneous fit of the susceptibility and magnetisation data to spin-Hamiltonian (1) afforded $J_{Cu–Re}$ = −0.45 cm^{-1}. The data cannot be fitted without including exchange between the Cu and Re metal ions. Thus, the experimental magnetic data suggests: (a) there is no magnetic interaction between the Cu^{II} centres (at least for the sensitivity of a SQUID magnetometer). (b) There is a small but finite antiferromagnetic interaction between the $Cu^{II}–Re^{IV}$ ions. (c) Analogous D_{Re} values to previously published Re^{IV} metal salts are observed for the encapsulated $ReBr_6^{2-}$ ions, due to retention of analogous/non-distorted structures. In order to probe these details further, we now turn to theory.

Theoretical calculations

CASSCF/NEVPT2 calculations performed on the $ReBr_6^{2-}$ guest in **3** suggests that the major contribution to D_{Re} comes from the spin–flip transition $|d_{yz/xz} \rightarrow d_{xy}|$. Due to the relatively weak π-donor nature of the Br ion, the splitting between the $d_{yz/xz}$ and d_{xy} orbitals is found to be rather small, facilitating strong in-plane anisotropy (Table S6 and Fig. S11, S12†).[30] In order to estimate the J_{Cu-Cu} and J_{Cu-Re} exchange interactions DFT calculations have been performed on complexes **1** and **3**. Calculations suggest no interaction between the two Cu^{II} ions in **1** and **3**, but a non-negligible antiferromagnetic J_{Cu-Re} = -0.15 cm^{-1} in **3** leading to an $S = \frac{1}{2}$ ground state (Table 1, see ESI for computational details†). Spin density analysis shows the exchange is primarily mediated *via* the $Re^{IV}–Br\cdots Cu^{II}$ pathway (Fig. S13†). Overlap integral calculations[31–35] between singly occupied molecular orbitals (SOMOs) of the paramagnetic ions, which helps in analysing the sign and magnitude of magnetic exchange interactions, reveal one moderately strong orbital interaction between the $Re^{IV}–Br\cdots Cu^{II}$ centres $(Cu(d_{x^2-y^2})|Br3|Re(d_{yz})$; Fig. 3, S14, Table S7†) leading to an antiferromagnetic interaction. In the other two possible interactions $(Cu(d_{x^2-y^2})||Re(d_{xz})$ and $Cu(d_{x^2-y^2})||Re(d_{xy}))$, the Re^{IV} magnetic orbitals $(d_{xz/xy})$ are not directly interacting with the $Cu^{II}(d_{x^2-y^2})$ orbital, rather they interact through the long, extended π/π* orbitals of L (Fig. S14 and Table S7†). The contribution from these two interactions to the magnetic exchange interaction is thus expected to be minimal. To further confirm the significance of the Br3 atoms in mediating the exchange

interaction, we have replaced Br1 and Br2 with point charges (Fig. S15†) and observe a minimal decrease in the magnitude of antiferromagnetic magnetic exchange interaction (-0.15 cm^{-1} to -0.12 cm^{-1}). This is also supported by natural bonding orbitals (NBOs) analysis,[36] where considerable donor → acceptor interactions are observed between hybrid $|4s^{0.37}4p_x^{0.63}|$ orbitals of Br3 and the empty 4s and 4p orbitals on Cu (Table S8†).

Conclusions

Lantern-like guest⊂$[M_2L_4]^{4+}$ coordination cages, normally associated with diamagnetic metals ions such as Pd^{II}, can also be made with paramagnetic M^{II} ions, here Cu^{II}, through simple self-assembly of four molar equivalents of the ligand molecule (L = 1,3-bis(3-ethynylpyridyl)benzene) with two molar equivalents of the corresponding metal salt, followed by one molar equivalent of guest, forming $[Cu^{II}_2L_4(H_2O)(OTf)_3]$(OTf)·MeCN (**1**), $ReBr_6 \subset [Pd^{II}_2L_4](BF_4)_2$ (**2**) and $ReBr_6 \subset [Cu^{II}_2L_4(OTf)_2]$ (**3**), respectively. Complex formation was confirmed by ESI-MS and ^{1}H NMR, both revealing solution stability. Magnetic measurements combined with theoretical calculations show that: (a) there is no magnetic interaction between the Cu^{II} ions in the "empty" $[Cu_2L_4]^{4+}$ cage, **1**. (b) The geometry of the encapsulated $[ReBr_6]^{2-}$ ion remains essentially unchanged with respect to its metal salt and thus the axial zero-field splitting parameter, D_{Re}, also remains the same. (c) The ingress of the $ReBr_6^{2-}$ ion induces a magnetic exchange interaction between the Re^{IV} guest and the Cu^{II} host, mediated primarily by the $Cu(d_{x^2-y^2})||Re(d_{yz})$ orbitals in the Re–Br⋯Cu pathway leading to dominant antiferromagnetic exchange and an $S = \frac{1}{2}$ ground state for the complex. This was confirmed by overlap integral calculations and NBOs analysis where significant donor-to-acceptor interactions are observed between hybrid $|4s^{0.37}4p_x^{0.63}|$ orbitals of the Br ions and the empty 4s, 4p orbitals of the Cu ions. The ability of paramagnetic host complexes to encapsulate paramagnetic guest complexes highlights some interesting possibilities for future work. These include: (1) the ability to switch on/off magnetic interactions through simple solution-based/redox chemistry, or through external perturbation, *e.g.* light, pressure, magnetic/electric fields. (2) To specifically design host frameworks able to isolate/stabilise unstable/reactive magnetic molecules or those with unusual geometries/coordination numbers. The structural and physical characterisation of such species will have potential application across a breadth of electron–spin based quantum technologies.
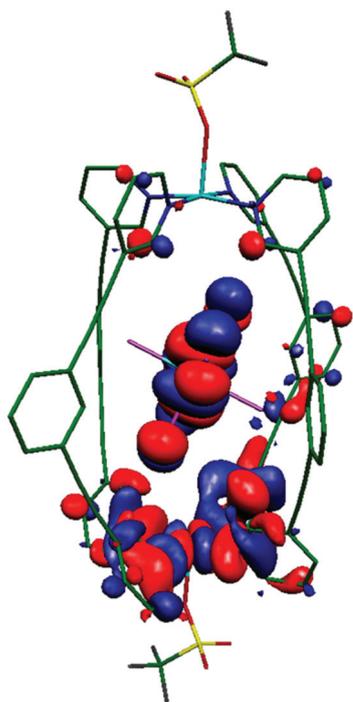
Fig. 3 Computed overlap integral showing the $Cu(d_{x^2-y^2})||Re(d_{yz})$ interaction in **3** mediating the strongest contribution to the antiferromagnetic exchange in the Re−Br⋯Cu moiety.

Author contributions

M. K. S., A. E. B., J. V., S. S. and J. M. L. performed the synthesis and characterisation. G. S. N. performed the XRD. P. J. L. and E. K. B. conceived the idea. All authors contributed to the writing of the manuscript.

Conflicts of interest

There are no conflicts to declare.

Acknowledgements

References

1 D. A. McMorran and P. J. Steel, *Angew Chem., Int. Ed.*, 1998, **37**, 3295–3297.

2 G. H. Clever, S. Tashiro and M. Shionoya, *Angew. Chem., Int. Ed.*, 2009, **48**, 7010–7012.

3 P. Liao, B. W. Langloss, A. M. Johnson, E. R. Knudsen, F. S. Tham, R. R. Julian and R. J. Hooley, *Chem. Commun.*, 2010, **46**, 4932–4934.

4 N. Kishi, Z. Li, K. Yoza, M. Akita and M. Yoshizawa, *J. Am. Chem. Soc.*, 2011, **133**, 11438–11441.

5 J. E. M. Lewis, E. L. Gavey, S. A. Cameron and J. D. Crowley, *Chem. Sci.*, 2012, **3**, 778–784.

6 W. M. Bloch, J. J. Holstein, W. Hiller and G. H. Clever, *Angew. Chem., Int. Ed.*, 2017, **56**, 8285–8289.

7 J. E. M. Lewis, A. Tarzia, A. J. P. White and K. E. Jelfs, *Chem. Sci.*, 2020, **11**, 677–683.

8 H. Lee, J. Tessarolo, D. Langbehn, A. Baksi, R. Herges and G. H. Clever, *J. Am. Chem. Soc.*, 2022, **144**, 3099–3105.

9 D. P. August, G. S. Nichol and P. J. Lusby, *Angew. Chem., Int. Ed.*, 2016, **55**, 15022–15026.

10 M. Yamashina, M. Akita, T. Hasegawa, S. Hayashi and M. Yoshizawa, *Sci. Adv.*, 2017, **3**, e1701126/1–e1701126/6.

11 B. Woods, R. D. M. Silva, C. Schmidt, D. Wragg, M. Cavaco, V. Neves, V. F. C. Ferreira, L. Gano, T. S. Morais, F. Mendes, J. D. G. Correia and A. Casini, *Bioconjugate Chem.*, 2021, **32**, 1399–1408.

12 V. Martí-Centelles, A. L. Lawrence and P. J. Lusby, *J. Am. Chem. Soc.*, 2018, **140**, 2862–2868.

13 J. Wang, T. A. Young, F. Duarte and P. J. Lusby, *J. Am. Chem. Soc.*, 2020, **142, 41**, 17743–17750.

14 Z. Li, N. Kishi, K. Yoza, M. Akita and M. Yoshizawa, *Chem. – Eur. J.*, 2012, **18**, 8358–8365.

15 A. J. Scott, J. Vallejo, A. Sarkar, L. Smythe, E. R. Marti, G. S. Nichol, W. T. Klooster, S. J. Coles, M. Murrie, G. Rajaraman, S. Piligkos, P. J. Lusby and E. K. Brechin, *Chem. Sci.*, 2021, **12**, 5134–5142.

16 G. A. Craig and M. Murrie, *Chem. Soc. Rev.*, 2015, **44**, 2135–2147.

17 A. Zabala-Lekuona, J. M. Seco and E. Colacio, *Coord. Chem. Rev.*, 2021, **441**, 213984.

18 R. Hussain, G. Allodi, A. Chiesa, E. Garlatti, D. Mitcov, A. Konstantatos, K. S. Pedersen, R. De Renzi, S. Piligkos and S. Carretta, *J. Am. Chem. Soc.*, 2018, **140**, 9814–9818.

19 M. Ohba, K. Yoneda, G. Agusti, M. C. Muñoz, A. B. Gaspar, J. A. Real, M. Yamasaki, H. Ando, Y. Nakao, S. Sakaki and S. Kitagawa, *Angew. Chem., Int. Ed.*, 2009, **48**, 4767–4771.

20 J. Vallejo, F. R. Fortea-Pérez, E. Pardo, S. Benmansour, I. Castro, J. Krzystek, D. Armentano and J. Cano, *Chem. Sci.*, 2016, **7**, 2286–2293.

21 G. J. Halder, C. J. Kepert, B. Moubaraki, K. S. Murray and J. D. Cashion, *Science*, 2002, **298**, 1762–1765.

22 M. Feng and M.-L. Tong, *Chem. – Eur. J.*, 2018, **24**, 7574–7594.

23 M. Atzori and R. Sessoli, *J. Am. Chem. Soc.*, 2019, **141**, 11339–11352.

24 J. Martínez-Lillo, J. Faus, F. Lloret and M. Julve, *Coord. Chem. Rev.*, 2015, **289–290**, 215–237.

25 C. H. Woodall, G. A. Craig, A. Prescimone, M. Misek, J. Cano, J. Faus, M. R. Probert, S. Parsons, S. Moggach, J. Martinez-Lillo, M. Murrie, K. V. Kamenev and E. K. Brechin, *Nat. Commun.*, 2016, **7**, 13870.

26 V. Minkiewicz, G. Shirane, B. Frazer, R. Wheeler and P. Dorain, *J. Phys. Chem. Solids*, 1968, **29**, 881–884.

27 D. P. August, G. S. Nichol and P. J. Lusby, *Angew. Chem., Int. Ed.*, 2016, **55**, 15022–15026.

28 SHAPE, version 2.0, continuous shape measures calculation; Electronic Structure Group, Universiat de Barcelona: Barcelona, Spain, 2010.

29 S. K. Singh and G. Rajaraman, *Nat. Commun.*, 2016, **7**, 10669.

30 D. J. Cutler, M. K. Singh, G. S. Nichol, M. Evangelisti, J. Schnack, L. Cronin and E. K. Brechin, *Chem. Commun.*, 2021, **57**, 8925–8928.

31 A. E. Dearle, D. J. Cutler, H. W. L. Fraser, S. Sanz, E. Lee, S. Dey, I. F. Diaz-Ortega, G. S. Nichol, H. Nojiri, M. Evangelisti, G. Rajaraman, J. Schnack, L. Cronin and E. K. Brechin, *Angew. Chem., Int. Ed.*, 2019, **58**, 16903–16906.

32 M. K. Singh and G. Rajaraman, *Inorg. Chem.*, 2019, **58**, 3175–3188.

33 M. K. Singh, T. Rajeshkumar, R. Kumar, S. K. Singh and G. Rajaraman, *Inorg. Chem.*, 2018, **57**, 1846–1858.

34 S. Hazra, S. Bhattacharya, M. K. Singh, L. Carrella, E. Rentschler, T. Weyhermueller, G. Rajaraman and S. Mohanta, *Inorg. Chem.*, 2013, **52**, 12881–12892.

35 J. P. Foster and F. Weinhold, *J. Am. Chem. Soc.*, 1980, **102**, 7211–7218.

36 M. K. Singh, N. Yadav and G. Rajaraman, *Chem. Commun.*, 2015, **51**, 17732–17735.